

Efficient Separation and Purification Method for Recovering Valuable Elements from Bismuth Telluride Refrigeration Chip Waste

Jiangling Zhu, Gang Wang,* Wenjun Zhu, Linrui Ou, Lin Zheng, Jie Zhang, Jinwei Chen, Jingong Pan, and Rulin Wang



Cite This: *ACS Omega* 2023, 8, 39222–39232

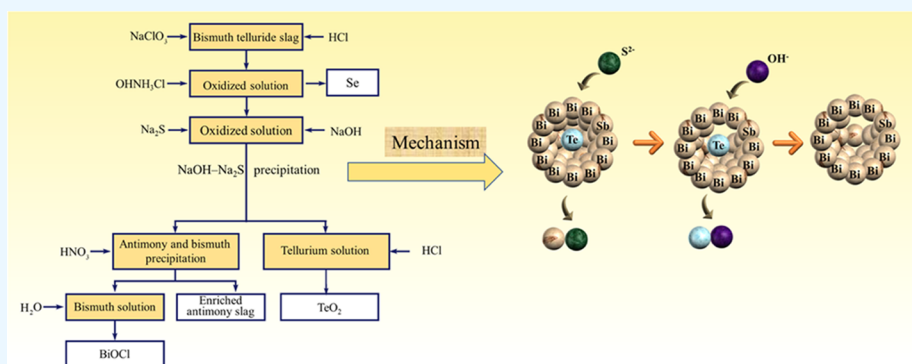


Read Online

ACCESS |

Metrics & More

Article Recommendations



ABSTRACT: Bismuth telluride and its alloys are widely utilized in thermoelectric refrigeration and power generation devices. Waste bismuth telluride-based cooling chips contain valuable elements; however, recycling processes for these materials remain underdeveloped due to their complexity. In this study, we developed a concise and efficient chemical method that does not require expensive reagents or equipment, enabling the separation and purification of tellurium, bismuth, selenium, and antimony from waste bismuth telluride-based cooling chips. Initially, the waste was leached with HCl and NaClO₃ to dissolve primary elements and recover 99.9% of selenium using hydroxylamine hydrochloride. Subsequently, Na₂S and NaOH were employed for precipitation and leaching, resulting in a solution containing tellurium. The precipitated residue was treated with HNO₃ to oxidize antimony into insoluble SbOH and dissolve bismuth completely. 99.8% of the bismuth telluride waste was dissolved via oxidative leaching through hydrolysis. A small amount of sodium sulfide reduced the precipitation percentage of tellurium from 11.9% to 7.5% in an alkaline solution, and the direct recovery percentage of tellurium in the form of TeO₂ exceeded 90%, while the purity of TeO₂ reached 99.9%. By adjusting the pH of the bismuth solution to 0.15, 98.9% of the bismuth was able to precipitate and be recovered as BiOCl, with the purity also reaching 99.9%. In summary, this study presents an efficient hydrometallurgical method for treating bismuth telluride waste and provides theoretical guidance for reagent dosage, demonstrating the significant potential for industrial applications.

1. INTRODUCTION

In 1950, the Bi₂Te₃-based thermoelectric materials with the Seebeck effect and the Peltier effect were discovered.¹ Presently, Bi₂Te₃ is the sole thermoelectric material that has been commercialized and extensively used in chip cooling, power generation, and infrared sensing applications.²

Bi₂Te₃-based thermoelectric materials consist of Bi₂Te₃ crystals and retain their inherent crystal structure characteristics after they incorporate doped elements. For example, doping with Sb and Se alters the physical properties while preserving the chemical properties akin to Bi₂Te₃ crystals. The bonding mechanism between Bi–Te atoms is covalent, while van der Waals forces govern Te–Te atom interactions, rendering the material prone to cleavage along the Te–Te bonding plane.³ The material's inferior mechanical properties lead to easy

fracturing, and during the cutting process of bismuth telluride rods and sheets, substantial waste is generated, resulting in material and energy losses.

Bismuth telluride sheets produce substantial waste at the end of their service life, primarily comprising tellurium, bismuth, selenium, and antimony. These elements exhibit a dispersed distribution, and their production is constrained by mineral

Received: June 27, 2023

Accepted: September 26, 2023

Published: October 10, 2023



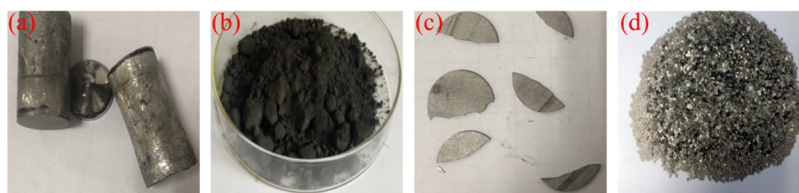


Figure 1. Waste from bismuth telluride cooling chips: (a) fractured crystal rods, (b) cutting powders, (c) broken crystal flakes, and (d) dysfunctional crystal grains.

availability. Consequently, it is vital to recover and separate tellurium, bismuth, selenium, and antimony from bismuth telluride waste to minimize waste and promote resource sustainability.⁴

Numerous physical and chemical processing techniques have been developed for the leaching and purification of tellurium.⁵ The pyrometallurgical method offers a straightforward process and a brief recovery period. However, within the anode slimes containing tellurium and copper, the formation of various compounds that inhibit tellurium dissolution typically results in a total extraction percentage of only 80%.⁶ Conversely, chemical methods are more cost-effective and provide higher leaching percentages. The leaching ratio of Te can reach 99% after oxidation with concentrated nitric acid and leaching with hydrochloric acid.⁷ In the case of acidic leaching solution containing tellurium and selenium, hydroxylamine hydrochloride serves as an effective reducing agent for separating tellurium and selenium, as it reduces selenium without affecting tellurium, thus achieving their separation.⁸

When dealing with mixed solid materials containing tellurium and metals like copper, direct alkali leaching is generally an inefficient method for recovering tellurium,^{9,10} as the recovery percentage is low and coprecipitation hinders complete leaching of impurities.¹¹ However, sulfide leaching significantly enhances the leaching percentage.¹² When leaching tellurium-containing alkaline residues, with a Na_2S concentration of 200 g/L, a temperature of 80 °C, an L/S ratio of 10:1 mL/g, and a leaching time of 60 min, 94.92% of tellurium is extracted.¹³ The dissolution of tellurium is governed by a combination of diffusion and chemical reactions. Te can be recovered from the leachate using Na_2S and Na_2SO_3 ,¹⁴ where Te is converted into TeS_4^{2-} and ultimately precipitated by Na_2SO_3 .¹⁵

Nitric acid is a highly effective agent for separating bismuth and antimony.¹⁶ The addition of nitric acid to a mixture of antimony and bismuth leads to the dissolution of bismuth in the form of Bi^{3+} , while antimony is oxidized into the insoluble compound SbOHN .¹⁷

Although the aforementioned methods have been proven effectively in recovering tellurium, bismuth, selenium, and antimony, individually, their direct application to recycle bismuth telluride waste is difficult due to its complex composition.⁶ These methods lack specificity and tend to yield products of a relatively low purity. Furthermore, the low valence and stability of tellurium and bismuth in bismuth telluride cooling chips make the direct acid leaching or alkali leaching methods ineffective at dissolving the material.^{9,10} In the case of the Na_2S leaching process, a high concentration of Na_2S results in substantial reagent consumption and generates sodium thioantimonate, a compound that requires additional processing to convert into the more commercially desirable antimony oxide, thus escalating operational costs.¹⁷ Moreover, due to the complex composition of the waste cooling chips, none of these methods can comprehensively recover and separate all the major

elements,^{5–17} leading to significant material wastage. Therefore, enhancing the recovery efficiency of tellurium while effectively recovering other elements and improving the purity of the product at the same time is an issue that requires resolution.

The recycling technology for bismuth telluride waste remains underdeveloped among most domestic enterprises, and theoretical studies and academic reports on waste recycling are limited. Incomplete recovery of high-value elements not only leads to reduced economic and social benefits but also contributes to environmental pollution.⁴ Consequently, the comprehensive recovery of bismuth telluride waste is crucial for decreasing the production cost of bismuth telluride and protecting the environment.

In this study, we examined the process order and conditions, proposing a novel approach for recycling waste bismuth telluride waste. Initially, the waste underwent oxidative leaching using HCl and NaClO_3 . Subsequently, hydroxylamine hydrochloride was employed to selectively reduce selenium, followed by the precipitation of antimony and bismuth using NaOH and Na_2S . HNO_3 was then utilized to treat the precipitated residue, retaining antimony in the residue and enabling the complete dissolution of bismuth and its eventual recovery through hydrolysis. This hydrometallurgical method selectively separates high-value elements Te, Bi, Se, and Sb from bismuth telluride waste, significantly enhancing the purity of tellurium and bismuth, thus providing both theoretical and dosage guidance for their recycling. The process has several advantages, including simplicity, brevity, high resource utilization efficiency, and the absence of the need for additional equipment, indicating the significant potential for its application in the recovery and treatment of bismuth telluride waste within the industry.

2. EXPERIMENTAL METHODS

2.1. Materials. The bismuth telluride powder materials used in the experiments were sourced from production waste and failed chips of bismuth telluride-based cooling chips supplied by domestic material providers. These production wastes and failed chips are primarily derived from fractured crystal rods, cutting powders, broken crystal flakes, and dysfunctional crystal grains (Figure 1). The bismuth telluride waste used in this experiment is a uniform mixture of the four materials mentioned above, which has been crushed using a grinder, with particle sizes ranging from 0.1 to 3 mm. All other chemical reagents (including hydrochloric acid, nitric acid, sodium hydroxide, and sodium sulfide) were of analytical grade purity and procured from local chemical suppliers without further purification.

2.2. Experimental Procedures and Equipment. Figure 2 presents a schematic illustration of the overall process. Initially, 10 g of waste slag was added to the reactor and heated in a temperature-controlled water bath. Upon reaching the desired temperature, HCl was added directly, followed by the addition of different volumes of 30 wt % NaClO_3 solution at a drip rate of 3 mL/min. Throughout the entire reaction process, the stirrer

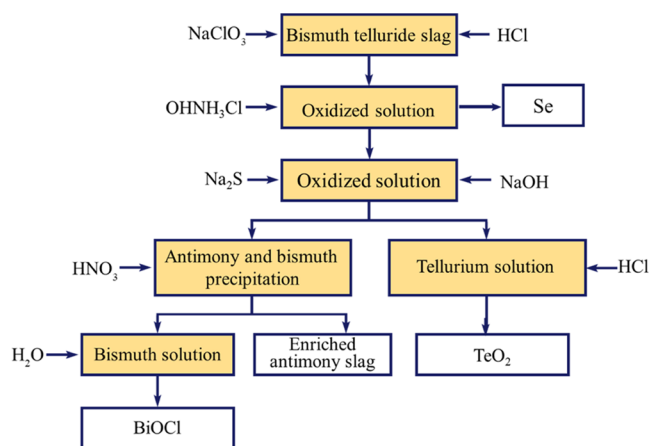


Figure 2. Schematic representation of the overall process.

was maintained at a rotational speed of 100 rpm. After the reaction was completed, the filtered liquid was treated with the required amount of hydroxylamine hydrochloride to reduce selenium. The solid precipitate was filtered out, and the appropriate volumes of NaOH and Na₂S solution were successively added. The precipitate was then filtered, dried at 70 °C for 8 h, and weighed. Subsequently, the required volume of HNO₃ was added to dissolve the solid precipitate obtained from NaOH–Na₂S precipitation, and the mixture was filtered. Finally, the necessary amounts of water and NaOH were added for dilution and hydrolysis. The wastewater generated by hydrolysis can be treated as industrial wastewater,¹⁸ and the elements in the wastewater can be recovered through adsorption.¹⁹

2.3. Characterization and Analyses. Inductively coupled plasma atomic emission spectrometry (ICP-OES 7600, Thermo Fisher Scientific) was employed to determine the elemental content of samples, leachates, and precipitates. pH measurements were conducted by using a pH meter (pHS-3E, INESA, China). An X-ray diffractometer (Empyrean, Panalytical B.V., NL) was utilized to scan the waste residue and precipitation at a speed of 1°/min within the 10–80° 2θ range for X-ray diffraction (XRD) pattern analysis.

3. RESULTS AND DISCUSSION

3.1. Characterization of the Bismuth Telluride Waste. The results of ICP-OES analysis are presented in Table 1. The waste material predominantly consists of four elements: Te (43.99%), Bi (45.52%), Sb (8.11%), and Se (1.92%).

Table 1. Elemental Composition of the Raw Material (%)

Bi (%)	Te (%)	Sb (%)	Se (%)
45.52	43.99	8.11	1.92

X-ray diffraction analysis indicates that the primary phase present in the raw material is Bi₂Te₃ (Figure 3). Additionally, the positions of Bi and Te in Bi₂Te₃ are substituted by Sb and Se, resulting in the formation of Bi_{0.5}Sb_{1.5}Te₃ and Bi_{1.8}Sb_{0.2}Se_{0.15}Te_{2.85} with analogous structures. Therefore, during thermodynamic analysis, the raw materials can be considered a mixture of Bi₂Te₃ doped with Sb₂Te₃, Bi₂Se₃, and Sb₂Se₃ for discussion.³

We have introduced the concept of the excess coefficient to provide a more accurate representation of the amount of reagent

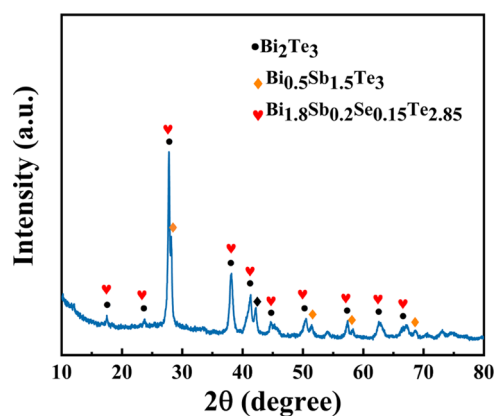


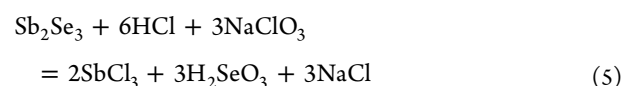
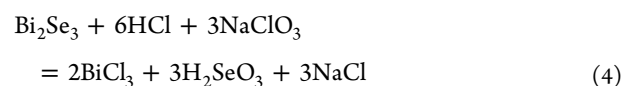
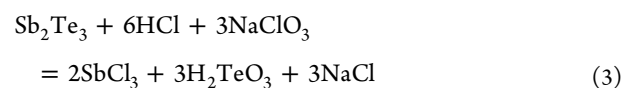
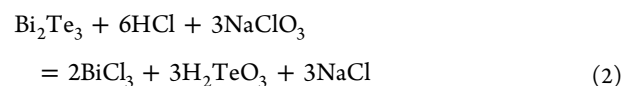
Figure 3. XRD patterns of the raw material slag.

used,¹⁴ which leads to an increased accuracy of the experiment. The calculation formula for the excess coefficient is as shown in eq 1

$$\text{excess coefficient} = \frac{\text{actual amount}}{\text{theoretical amount}} \quad (1)$$

The actual amount refers to the amount of reagents actually used in the experiment, while the theoretical amount is the required amount calculated based on the chemical reaction equation.

3.2. NaClO₃ Oxidative Leaching. **3.2.1. Effect of Oxidation Leaching Temperature and Thermodynamic Analyses.** Sodium chlorate is a potent oxidizing agent. Upon the addition of sodium chlorate to the solution, Bi and Sb dissolve in the forms Bi³⁺ and Sb³⁺, while Te is converted into TeO₃²⁻. The main reactions in the oxidative leaching process are shown in eqs 2–5.^{20,21}



In order to predict the thermodynamic trend of the reaction during oxidative leaching, the variations of the Gibbs free energy (ΔG) for eqs 2–5 were calculated and are plotted in Figure 4a based on the thermodynamic data from Hsc6.0. The smaller ΔG values for eqs 2 and 3 compared to eqs 4 and 5 suggest that Te is more readily oxidized and leached than Se and that Te is oxidized earlier than Se from a thermodynamic perspective.

Figure 4b demonstrates the effect of the temperature on the oxidative dissolution of the waste. Based on the ratio of the total weight of the residual solid after the reaction to the initial mass, we calculated the solid dissolution leaching percentage and present it in Figure 4b. The dissolution remained relatively constant at over 98% between 15 and 60 °C, reaching a peak of 99.8% at 50 °C. However, when the temperature exceeded 50

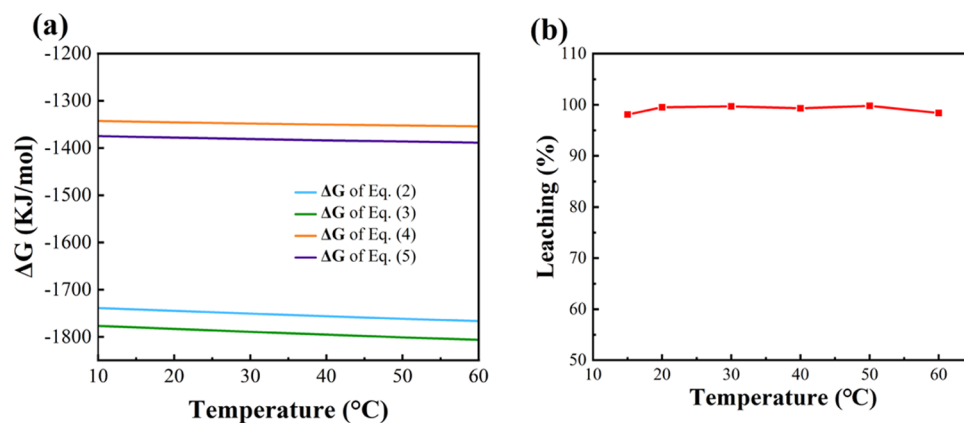


Figure 4. (a) ΔG of equations and (b) effect of oxidation temperature on the leaching (excess coefficient of NaClO_3 of 1 and time of 20 min).

°C, the dissolution percentage decreased due to excessive volatilization of hydrochloric acid, resulting in wasted oxidant and reduced leaching efficiency. Furthermore, the thermodynamic analysis presented in Figure 4a indicates that ΔG of the reaction (eqs 2–5) was not significantly impacted by temperature changes. It was also observed that due to the exothermic reaction, the system temperature would rise beyond the set value.

3.2.2. Effect of NaClO_3 Dosage. The oxidation reaction occurs rapidly, and a one-time addition would result in significant waste due to side reactions. Therefore, NaClO_3 was added dropwise to achieve oxidative dissolution of the raw material. Figure 5 illustrates the leaching efficiency of each element in 10 g of raw material after 20 min of reaction at 50 °C.

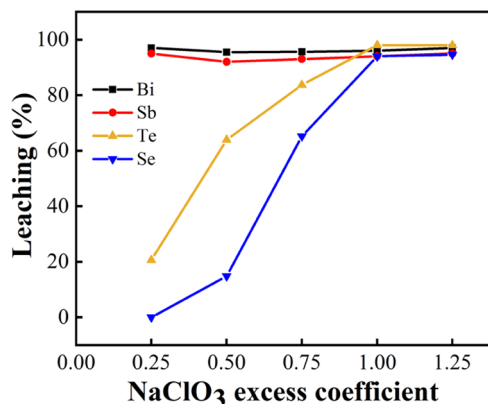


Figure 5. Effect of NaClO_3 dosage on Bi, Te, Sb, and Se leaching (reaction temperature of 50 °C and time of 20 min).

According to eqs 2–5, the complete dissolution of 10 g of bismuth telluride waste requires 4 g of NaClO_3 , and the excess coefficient of NaClO_3 was calculated and is presented in Figure 5. The elements, Bi, Sb, Te, and Se, were successively oxidized and dissolved in the specific order. When 1 g of NaClO_3 was added, 97% of bismuth and 95% of antimony were dissolved, whereas only 20% of Te was dissolved and Se remained undissolved. The dissolution of Te and Se increased gradually with the addition of NaClO_3 . Notably, when the NaClO_3 dosage was 4 g and the excess coefficient of NaClO_3 reached 1.00, 98% of Te and 94% of Se were dissolved. Further addition of NaClO_3 would increase the process cost. Therefore, an excess coefficient

of 1.00 was selected as the optimal condition for the NaClO_3 dosage.

To investigate the specific process, the main substances considered in the Bi–Te– H_2O system were Bi_2Te_3 , BiCl_3 , Te, H_2TeO_3 , H_2TeO_4 , and H_2O . The Eh–pH diagram was created by using HSC6.0 (Figure 6). At 25 °C, as the pH decreased

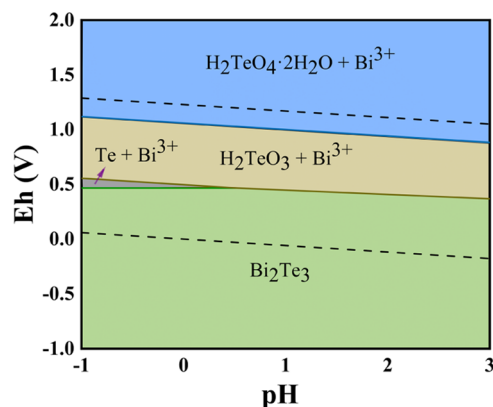


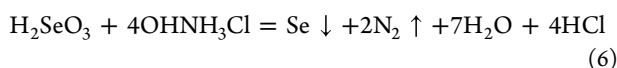
Figure 6. Potential–pH diagram of the Te–Bi– H_2O system at 25 °C.

below 0, the potential increased, causing leaching of Bi in the form of Bi^{3+} and oxidation of tellurium into its elemental form, which was not leached. A further increase in potential led to the oxidation of tellurium to TeO_3^{2-} , and the material dissolved. Finally, TeO_3^{2-} is further oxidized to TeO_4^{2-} . TeO_4^{2-} is insoluble in alkaline solutions, which reduces the leaching and recovery of tellurium. Therefore, controlling the oxidation of tellurium is crucial.^{9,22}

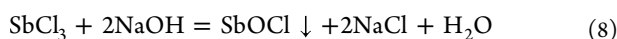
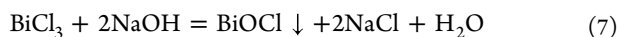
Under the experimental conditions with concentrated hydrochloric acid (12 mol/L), the oxidative leaching of Te occurred in two stages. Initially, Te in Bi_2Te_3 was oxidized to its elemental form, resulting in the leaching of Bi as Bi^{3+} . This explains why Bi was the first to be oxidized and leached when the amount of the oxidant was low. Subsequently, with the increase in the amount of oxidant, Te was dissolved in the form of TeO_3^{2-} .

3.3. Separation and Recovery of Selenium. The main-group elements tellurium and selenium have similar chemical properties. To minimize tellurium loss during reduction and facilitate tellurium–selenium separation, this study employed hydroxylamine hydrochloride for the selective reduction of tetravalent selenium. In the first step, hydroxylamine hydrochloride was added to the solution in an excess amount of 5

times the selenium content, resulting in the recovery of 99% of selenium, while the loss of tellurium, bismuth, and antimony was negligible (eq 6).⁸



3.4. NaOH–Na₂S Precipitation. NaOH and Na₂S were added to the leaching solution obtained in the previous step, resulting in a neutralization reaction between the base and the acid. Consequently, the pH increased, causing Bi and Sb to precipitate in the form of oxychlorides. Meanwhile, Te formed soluble tellurium, which dissolved in the alkaline solution. The main reactions are shown in eqs 7–9²¹



3.4.1. Effect of NaOH Dosage. After the addition of NaOH to the solution, a neutralization reaction occurred. Figure 7 depicts

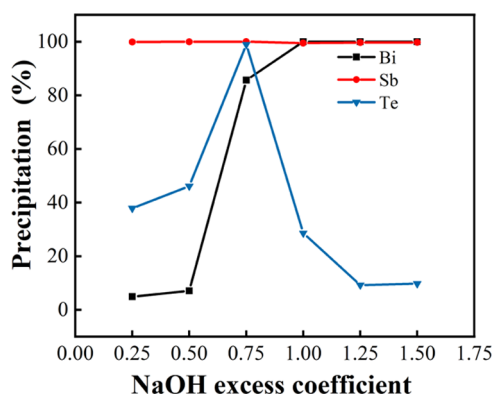


Figure 7. Effect of NaOH dosage on the precipitation (per 10 mL of the leaching solution).

the precipitation percentage of each element in 10 mL of leachate upon the addition of varying weights of NaOH (1, 2, 3, 4, 5, and 6 g). The excess coefficient of NaOH was calculated based on the quantity required to neutralize hydrochloric acid. Upon adding 1 g of NaOH, 99.9% of Sb and 4.8% of Bi were precipitated. As the amount of NaOH increased, the precipitation of Te reached a maximum of 98.9% at 3 g, followed by a gradual decrease. With the addition of 4 g of NaOH, the precipitation percentages of Bi and Te were 99.9 and 28.5%, respectively. By increasing the NaOH amount to 5 g, the precipitation percentages of Bi and Sb remained over 99.9%, while that of Te decreased to 11.9%. Consequently, 5 g of NaOH was chosen as the optimal amount for subsequent experiments, with an excess coefficient of 1.25.

As NaOH was added, the pH of the solution increased, causing Sb and Bi to undergo sequential hydrolysis. In this solution, pH and Cl⁻ concentrations were the primary factors influencing the precipitation of Sb and Bi. The main reactions are shown in Table 2 (eqs 10–24).^{23–26}

The reaction equilibrium constants related to eqs 10–24 are shown in Table 3.²⁶

Bi³⁺ in the solution can form four types of precipitates: BiOCl, Bi₂O₃, Bi(OH)₃, and BiOOH. Let [Bi³⁺] represent the concentration of Bi³⁺ in the solution and [Bi³⁺]_T denote the

total concentration of bismuth in the solution. Set pH = X and lg[Cl⁻] = Y.

It is assumed that all precipitates are BiOCl.

$$K_{21} = \frac{[\text{H}^+]^2}{[\text{Bi}^{3+}][\text{Cl}^-]} \rightarrow [\text{Bi}^{3+}]_{\text{BiOCl}} = \frac{[\text{H}^+]^2}{K_{21}[\text{Cl}^-]} = 10^{-2X-6.44-Y} \quad (25)$$

It is assumed that all of the precipitates are Bi₂O₃.

$$K_{22} = \frac{[\text{H}^+]^6}{[\text{Bi}^{3+}]^2} \rightarrow [\text{Bi}^{3+}]_{\text{Bi}_2\text{O}_3} = \left(\frac{[\text{H}^+]^6}{K_{22}} \right)^{0.5} = 10^{-3X-4.575} \quad (26)$$

It is assumed that all precipitates are Bi(OH)₃.

$$K_{\text{sp}} = [\text{Bi}^{3+}][\text{OH}^-]^3 \rightarrow [\text{Bi}^{3+}]_{\text{Bi(OH)}_3} = \frac{K_{\text{sp}}}{[\text{OH}^-]^3} = 10^{-3X+11.48} \quad (27)$$

It is assumed that all precipitates are BiOOH.

$$K_{24} = \frac{[\text{H}^+]^3}{[\text{Bi}^{3+}]} \rightarrow [\text{Bi}^{3+}]_{\text{BiOOH}} = \frac{[\text{H}^+]^3}{K_{24}} = 10^{-3X+4.094} \quad (28)$$

The initial concentrations of H⁺ and Cl⁻ were both 12 mol/L. The concentration hierarchy is as follows: [Bi³⁺]_{BiOCl} < [Bi³⁺]_{Bi₂O₃} < [Bi³⁺]_{BiOOH} < [Bi³⁺]_{Bi(OH)₃}. Consequently, the earliest product of bismuth hydrolysis is BiOCl, followed by Bi₂O₃. The formation of BiOOH requires a higher pH. Therefore, eq 21 represents the most significant reactions taking place, and the concentration of Bi³⁺ in the solution can be determined using this equation

$$K_{21} = \frac{[\text{H}^+]^2}{[\text{Bi}^{3+}][\text{Cl}^-]} \rightarrow [\text{Bi}^{3+}] = \frac{[\text{H}^+]^2}{K_{21}[\text{Cl}^-]} = 10^{-2X-6.44-Y} \quad (29)$$

Sb³⁺ can form four forms of precipitation: SbOCl, Sb₄O₅Cl₂, Sb₂O₃, and Sb(OH)₃.

It is assumed that all precipitates are SbOCl.

$$K_{14} = \frac{[\text{H}^+]^2}{[\text{Sb}^{3+}][\text{Cl}^-]} \rightarrow [\text{Sb}^{3+}]_{\text{SbOCl}} = \frac{[\text{H}^+]^2}{K_{14}[\text{Cl}^-]} = 10^{-2X-6.51-Y} \quad (30)$$

It is assumed that all precipitates are Sb₄O₅Cl₂.

$$K_{15} = \frac{[\text{H}^+]^{10}}{[\text{Sb}^{3+}]^4[\text{Cl}^-]^2} \rightarrow [\text{Sb}^{3+}]_{\text{Sb}_4\text{O}_5\text{Cl}_2} = \left(\frac{[\text{H}^+]^{10}}{K_{15}[\text{Cl}^-]^2} \right)^{0.25} = 10^{-2.5X-7.85-0.5Y} \quad (31)$$

It is assumed that all precipitates are Sb₂O₃.

$$K_{16} = \frac{[\text{H}^+]^6}{[\text{Sb}^{3+}]^2} \rightarrow [\text{Sb}^{3+}]_{\text{Sb}_2\text{O}_3} = \left(\frac{[\text{H}^+]^6}{K_{16}} \right)^{0.5} = 10^{-3X-4.91} \quad (32)$$

It is assumed that all of the precipitates are Sb(OH)₃.

$$K_{\text{sp}} = [\text{Sb}^{3+}][\text{OH}^-]^3 \rightarrow [\text{Sb}^{3+}]_{\text{Sb(OH)}_3} = \frac{K_{\text{sp}}}{[\text{OH}^-]^3} = 10^{-3X+0.15} \quad (33)$$

Table 2. Reactions in Solution during the Precipitation Process

reaction equation	reaction equilibrium constant
$\text{Sb}^{3+} + m\text{Cl}^- = \text{SbCl}_m^{3-m}$	$\beta = \frac{[\text{SbCl}_m^{3-m}]}{([\text{Sb}^{3+}][\text{Cl}^-]^m)} (m = 1 - 6) \quad (10)$
$\text{Sb}^{3+} + n\text{OH}^- = \text{Sb}(\text{OH})_n^{3-n}$	$\beta = \frac{[\text{Sb}(\text{OH})_n^{3-n}]}{[\text{Sb}^{3+}][\text{OH}^-]^n} (n = 1 - 4) \quad (11)$
$\text{Sb}^{3+} + \text{H}_2\text{O} = \text{SbO}^+ + 2\text{H}^+$	$K_{12} = \frac{[\text{SbO}^+][\text{H}^+]^2}{[\text{Sb}^{3+}]} \quad (12)$
$\text{Sb}^{3+} + 2\text{H}_2\text{O} = \text{SbO}_2^- + 4\text{H}^+$	$K_{13} = \frac{[\text{SbO}_2^-][\text{H}^+]^4}{[\text{Sb}^{3+}]} \quad (13)$
$\text{Sb}^{3+} + \text{Cl}^- + \text{H}_2\text{O} = \text{SbOCl}(\text{s}) + 2\text{H}^+$	$K_{14} = \frac{[\text{H}^+]^2}{[\text{Sb}^{3+}][\text{Cl}^-]} \quad (14)$
$4\text{Sb}^{3+} + 2\text{Cl}^- + 5\text{H}_2\text{O} = \text{Sb}_4\text{O}_5\text{Cl}_2(\text{s}) + 10\text{H}^+$	$K_{15} = \frac{[\text{H}^+]^{10}}{[\text{Sb}^{3+}]^4[\text{Cl}^-]^2} \quad (15)$
$2\text{Sb}^{3+} + 3\text{H}_2\text{O} = \text{Sb}_2\text{O}_3(\text{s}) + 6\text{H}^+$	$K_{16} = \frac{[\text{H}^+]^6}{[\text{Sb}^{3+}]^2} \quad (16)$
$\text{Sb}^{3+} + 3\text{OH}^- = \text{Sb}(\text{OH})_3(\text{s})$	$K_{\text{sp}} = [\text{Sb}^{3+}][\text{OH}^-]^3 \quad (17)$
$\text{Bi}^{3+} + i\text{Cl}^- = \text{BiCl}_i^{3-i}$	$\beta_i = \frac{[\text{BiCl}_i^{3-i}]}{[\text{Bi}^{3+}][\text{Cl}^-]^i} (i = 1 - 6) \quad (18)$
$\text{Bi}^{3+} + j\text{OH}^- = \text{Bi}(\text{OH})_j^{3-j}$	$\beta_j = \frac{[\text{Bi}(\text{OH})_j^{3-j}]}{[\text{Bi}^{3+}][\text{OH}^-]^j} (j = 1 - 4) \quad (19)$
$\text{Bi}^{3+} + \text{H}_2\text{O} = \text{BiO}^+ + 2\text{H}^+$	$K_{20} = \frac{[\text{BiO}^+][\text{H}^+]^2}{[\text{Bi}^{3+}]} \quad (20)$
$\text{Bi}^{3+} + \text{Cl}^- + \text{H}_2\text{O} = \text{BiOCl}(\text{s}) + 2\text{H}^+$	$K_{21} = \frac{[\text{H}^+]^2}{[\text{Bi}^{3+}][\text{Cl}^-]} \quad (21)$
$2\text{Bi}^{3+} + 3\text{H}_2\text{O} = \text{Bi}_2\text{O}_3(\text{s}) + 6\text{H}^+$	$K_{22} = \frac{[\text{H}^+]^6}{[\text{Bi}^{3+}]^2} \quad (22)$
$\text{Bi}^{3+} + 3\text{OH}^- = \text{Bi}(\text{OH})_3(\text{s})$	$K_{\text{sp}} = [\text{Bi}^{3+}][\text{OH}^-]^3 \quad (23)$
$\text{Bi}^{3+} + 2\text{H}_2\text{O} = \text{BiOOH}(\text{s}) + 3\text{H}^+$	$K_{24} = \frac{[\text{H}^+]^3}{[\text{Bi}^{3+}]} \quad (24)$

Table 3. Reaction Equilibrium Constants

complex	value	complex	value
SbCl_2^+	$10^{2.26}$	BiCl_6^{3-}	$10^{7.09}$
SbCl_2^+	$10^{3.49}$	$\text{Bi}(\text{OH})_2^+$	$10^{12.7}$
SbCl_3	$10^{4.18}$	$\text{Bi}(\text{OH})_2^+$	$10^{15.8}$
SbCl_4^-	$10^{4.72}$	$\text{Bi}(\text{OH})_4^-$	$10^{35.2}$
SbCl_5^{2-}	$10^{4.72}$	K_{12}	$10^{-1.6}$
SbCl_6^{3-}	$10^{4.11}$	K_{13}	$10^{-11.32}$
$\text{Sb}(\text{OH})_2^+$	$10^{14.61}$	K_{14}	$10^{6.51}$
$\text{Sb}(\text{OH})_2^+$	$10^{24.3}$	K_{15}	$10^{31.4}$
$\text{Sb}(\text{OH})_3$	$10^{36.7}$	K_{16}	$10^{9.82}$
$\text{Sb}(\text{OH})_4^-$	$10^{38.3}$	K_{17}	$10^{-42.15}$
BiCl_2^+	$10^{2.35}$	K_{20}	$10^{1.39}$
BiCl_2^+	$10^{4.4}$	K_{21}	$10^{6.44}$
BiCl_3	$10^{5.45}$	K_{22}	$10^{9.15}$
BiCl_4^-	$10^{6.65}$	K_{23}	$10^{-30.52}$
BiCl_5^{2-}	$10^{7.29}$	K_{24}	$10^{-4.094}$

The initial concentrations of H^+ and Cl^- were both 12 mol/L. The concentration hierarchy is as follows: $[\text{Sb}^{3+}]_{\text{Sb}_4\text{O}_5\text{Cl}_2} < [\text{Sb}^{3+}]_{\text{SbOCl}} < [\text{Sb}^{3+}]_{\text{Sb}_2\text{O}_3} < [\text{Sb}^{3+}]_{\text{Sb}(\text{OH})_3}$. Consequently, $\text{Sb}_4\text{O}_5\text{Cl}_2$ is the first product of antimony hydrolysis, followed by SbOCl , Sb_2O_3 , and $\text{Sb}(\text{OH})_3$. Therefore, eq 15 represents the

most significant reactions taking place, and the concentration of

Bi^{3+} in the solution can be determined by using this equation

$$K_{15} = \frac{[\text{H}^+]^{10}}{[\text{Sb}^{3+}]^4[\text{Cl}^-]^2} \rightarrow [\text{Sb}^{3+}] = \left(\frac{[\text{H}^+]^{10}}{K_{15}[\text{Cl}^-]^2} \right)^{0.25} = 10^{-2.5X-7.85-0.5Y} \quad (34)$$

As calculated above

$$K_{12} = \frac{[\text{SbO}^+][\text{H}^+]^2}{[\text{Sb}^{3+}]} \rightarrow [\text{SbO}^+] = \frac{K_{12}[\text{Sb}^{3+}]}{[\text{H}^+]^2} = 10^{-0.5X-9.45-0.5Y} \quad (35)$$

According to these calculations, the results can be obtained as follows

$$\begin{aligned}
 [\text{Sb}^{3+}]_{\text{T}} &= [\text{Sb}^{3+}] + [\text{SbO}^+] + [\text{SbO}_2^-] + [\text{SbCl}^{2+}] \\
 &+ [\text{SbCl}_2^+] + [\text{SbCl}_3] + [\text{SbCl}_4^-] + [\text{SbCl}_5^{5-}] \\
 &+ [\text{SbCl}_6^{3-}] + [\text{Sb}(\text{OH})^{2+}] + [\text{Sb}(\text{OH})_2^+] \\
 &+ [\text{Sb}(\text{OH})_4^-] \\
 &= 10^{-2.5X-7.85-0.5Y} + 10^{-0.5X-9.45-0.5Y} \\
 &+ 10^{1.5X-19.17-0.5Y} + 10^{-2.5X-5.59+0.5Y} \\
 &+ 10^{-2.5X-4.36+1.5Y} + 10^{-2.5X-3.67+2.5Y} \\
 &+ 10^{-2.5X-3.13+3.5Y} + 10^{-2.5X-3.13+4.5Y} \\
 &+ 10^{-2.5X-3.74+5.5Y} + 10^{-1.5X-7.24-0.5Y} \\
 &+ 10^{-0.5X-11.55-0.5Y} + 10^{1.5X-25.55-0.5Y}
 \end{aligned} \quad (36)$$

$$\begin{aligned}
 [\text{Bi}^{3+}]_{\text{T}} &= [\text{Bi}^{3+}] + [\text{BiO}^+] + [\text{BiCl}^{2+}] + [\text{BiCl}_2^+] \\
 &+ [\text{BiCl}_3] + [\text{BiCl}_4^-] + [\text{BiCl}_5^{2-}] + [\text{BiCl}_6^{3-}] \\
 &+ [\text{Bi}(\text{OH})^{2+}] + [\text{Bi}(\text{OH})_2^+] + [\text{Bi}(\text{OH})_4^-] \\
 &= 10^{-2X-6.44-Y} + 10^{-5.04-Y} + 10^{-2X-4.09} \\
 &+ 10^{-2X-2.04+Y} + 10^{-2X-0.99+2Y} \\
 &+ 10^{-2X+0.21+3Y} + 10^{-2X+0.85+4Y} \\
 &+ 10^{-2X+0.65+5Y} + 10^{-X-7.74-Y} + 10^{-18.64-Y} \\
 &+ 10^{2X-27.24-Y}
 \end{aligned} \quad (37)$$

The obtained results are illustrated in Figure 8, where each distinct color corresponds to the concentration of the ions in the

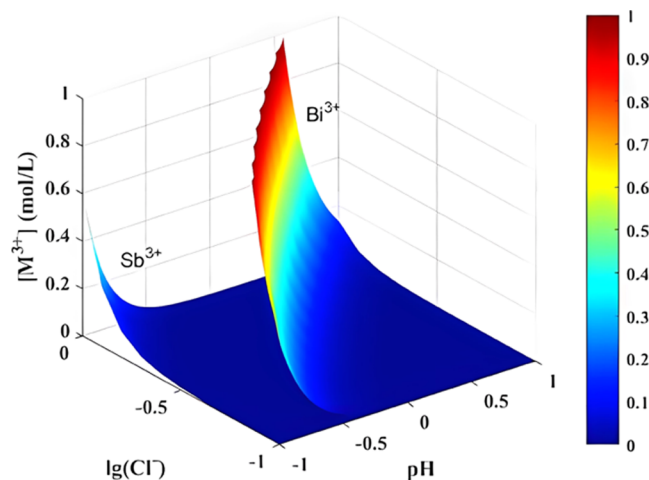
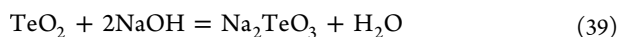


Figure 8. Concentrations of Sb and Bi in a chloride-containing acid solution.

solution. Transitioning from red to blue indicates a decrease in ion concentration from 1 to 0 mol/L. Sb will precipitate at a lower pH and a lower chloride ion concentration than Bi. Consequently, when a small quantity of sodium hydroxide is added, Sb will precipitate first, leading to a higher precipitation percentage of Sb at the beginning of the reaction compared to that of Bi.



Upon the addition of NaOH, tellurite acid yielded a tellurium dioxide precipitate (eq 38). As the amount of sodium hydroxide increased, tellurium dioxide dissolved in the form of TeO_3^{2-} (eq 39), causing precipitation to decrease. This process resulted in the tellurium precipitation percentage initially increasing and

then decreasing. Finally, sodium hydroxide was added to the obtained tellurium-containing solution, enabling the recovery of over 99% of tellurium by precipitation. In general, the direct recovery percentage of tellurium in the form of TeO_2 exceeded 90%, demonstrating promising prospects for industrial application.

3.4.2. Effect of Na_2S Dosage. The addition of sodium hydroxide alone cannot facilitate the leaching of certain portions of tellurium. As shown in Figure 9, the addition of 0.01 g of Na_2S

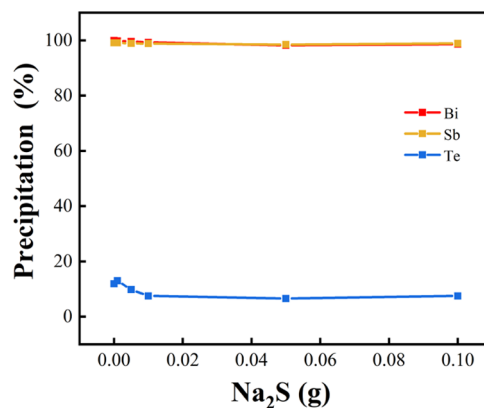


Figure 9. Effect of the Na_2S dosage on precipitation (per 10 mL of leaching solution).

per 10 mL of leaching solution can decrease the tellurium precipitation percentage from 11.9 to 7.5% and significantly enhance the recovery percentage of tellurium. The potential reason for this occurrence could be the complexation reaction of sodium sulfide with antimony and bismuth.^{27,28} In the minor portion of bismuth and antimony involved in the reaction, bismuth may reprecipitate in the form of Bi_2S_3 (eq 40),²⁶ with the ΔG of eq 40 being -222.353 kJ/mol at 25 °C. A small amount of antimony may dissolve in the form of Na_3SbS_3 ,²⁹ causing local concentration fluctuations by redissolving the surface of the solid precipitated particles (Figure 10). In this

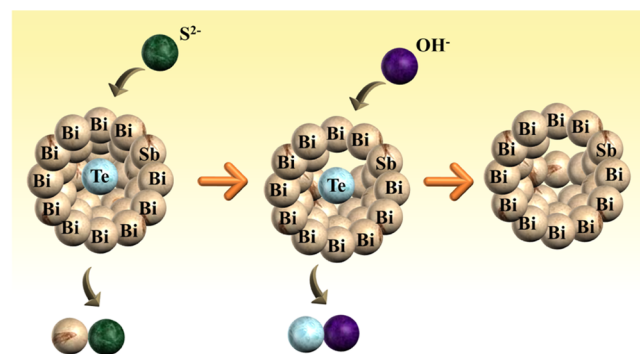


Figure 10. Schematic representation of the sodium sulfide mechanism.

process, the encapsulated tellurium reacted with OH^- to form soluble tellurium salts that entered the solution (eq 39). Consequently, the tellurium content in the antimony–bismuth precipitate decreased, leading to an improvement in the purity of antimony–bismuth. Based on these findings, we added 0.01 g of Na_2S per 10 mL of leaching solution in this step for subsequent leaching experiments. Due to the pH range of 4–6 for tellurium hydrolytic precipitation (Figure 11) and the fact that bismuth can hydrolyze at a pH of 0–1 (Figure 13), tellurium in the

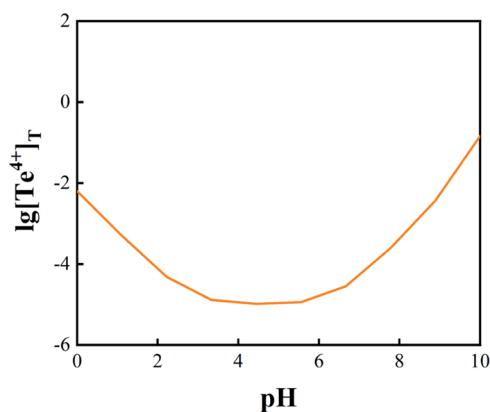
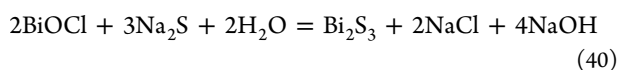


Figure 11. Effect of the pH on the hydrolysis of tellurium.

subsequent bismuth precipitation can be removed through hydrolysis.



Upon obtaining a tellurium leaching solution, we added a suitable quantity of HCl to initiate tellurium recovery. The primary reactions during this process are shown in Table 4.^{26,30}

Equations 41–44 lead to the following conclusions

$$\lg k_{41} = \lg[\text{H}_2\text{TeO}_3] - \text{pH} - \lg[\text{H}_3\text{TeO}_3^+] \quad (45)$$

$$\lg k_{42} = \lg[\text{H}_2\text{TeO}_3] + \text{pH} - \lg[\text{HTeO}_3^-] \quad (46)$$

$$\lg k_{43} = \lg[\text{H}_2\text{TeO}_3] + 2\text{pH} - \lg[\text{TeO}_3^{2-}] \quad (47)$$

$$\lg k_{44} = \lg[\text{H}_2\text{TeO}_3] \quad (48)$$

Subsequently, the concentrations of each hydrolyzed species can be determined as follows

$$[\text{H}_3\text{TeO}_3^+] = 10^{\lg k_{44} - \text{pH} - \lg k_{41}} \quad (49)$$

$$[\text{HTeO}_3^-] = 10^{\lg k_{44} + \text{pH} - \lg k_{42}} \quad (50)$$

$$[\text{TeO}_3^{2-}] = 10^{\lg k_{44} + 2\text{pH} - \lg k_{43}} \quad (51)$$

$$[\text{H}_2\text{TeO}_3] = 10^{\lg k_{44}} \quad (52)$$

Ultimately, the total concentration of all Te^{4+} -hydrolyzed species in the solution can be calculated as follows

$$\begin{aligned} [\text{Te}^{4+}]_T &= [\text{H}_3\text{TeO}_3^+] + [\text{TeO}_3^{2-}] + [\text{HTeO}_3^-] \\ &\quad + [\text{H}_2\text{TeO}_3] \\ &= 10^{\lg k_{31} - \text{pH} - \lg k_{28}} + 10^{\lg k_{31} + \text{pH} - \lg k_{29}} \\ &\quad + 10^{\lg k_{31} + 2\text{pH} - \lg k_{30}} + 10^{\lg k_{31}} \\ &= \log(10^{-2.2 - \text{pH}} + 10^{-20.97 + 2\text{pH}} + 10^{-11.41 + \text{pH}} \\ &\quad + 10^{-5.03}) \end{aligned} \quad (53)$$

Figure 11 presents the results, indicating that tellurium can be fully hydrolyzed in the pH range of 4–6. Subsequently, HCl was added to the acquired tellurium-containing solution, and the pH was adjusted to 5, yielding a recovery of over 99% of tellurium by precipitation. Overall, the direct recovery of tellurium in the form of TeO_2 exceeded 90%. Additionally, the impurity content within TeO_2 was exceedingly low, with an achievable purity of up to 99.9%.

3.5. Separation and Recovery of Antimony and Bismuth.

3.5.1. HNO_3 Dissolution and Leaching. 3 g of Bi–Sb precipitation obtained in the previous step was placed into a beaker, and a specific amount of nitric acid (68 wt %) was added. Nitric acid reacted with bismuth oxychloride, dissolving Bi in the form of Bi^{3+} (eq 54),³¹ while oxidizing Sb to insoluble antimony(III) oxide hydroxide nitrate (Sb(III)OHN),¹⁷ resulting in the formation of antimony-containing precipitates. As shown in Figure 12, after the addition of 3 mL of nitric acid,

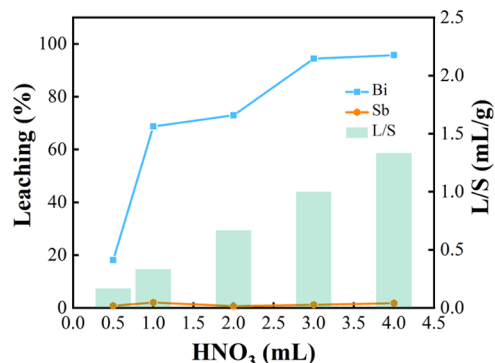


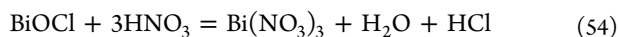
Figure 12. Effect of the HNO_3 dosage on leaching.

95.7% of bismuth could be directly dissolved and separated, while Sb remained nearly insoluble in nitric acid, facilitating the separation of bismuth and antimony. However, due to the low liquid–solid ratio at this stage, the ratio was 1.0 mL/g when 3 mL of HNO_3 was added, causing the concentration of bismuth in the solution to be excessively high. Consequently, bismuth

Table 4. Reactions in Solution during the Tellurium Precipitation Process

reaction equation	reaction equilibrium constant	value
$\text{H}_3\text{TeO}_3^+ = \text{H}_2\text{TeO}_3 + \text{H}^+$	$K_{41} = \frac{[\text{H}_2\text{TeO}_3][\text{H}^+]}{[\text{H}_3\text{TeO}_3^+]}$ (41)	$10^{-2.83}$
$\text{HTeO}_3^- + \text{H}^+ = \text{H}_2\text{TeO}_3$	$K_{42} = \frac{[\text{H}_2\text{TeO}_3]}{[\text{HTeO}_3^-][\text{H}^+]}$ (42)	$10^{6.38}$
$\text{TeO}_3^{2-} + 2\text{H}^+ = \text{H}_2\text{TeO}_3$	$K_{43} = \frac{[\text{H}_2\text{TeO}_3]}{[\text{TeO}_3^{2-}][\text{H}^+]^2}$ (43)	$10^{15.94}$
$\text{TeO}_2(\text{s}) + \text{H}_2\text{O} = \text{H}_2\text{TeO}_3$	$K_{44} = [\text{H}_2\text{TeO}_3]$ (44)	$10^{-5.03}$

experienced hydrolytic precipitation during filtration and washing, limiting the leaching percentage to 95.7%.



3.5.2. Bismuth Hydrolysis. Bismuth existed as Bi^{3+} ions in the solution obtained in the previous step. By adding deionized water, bismuth can be precipitated and recovered in the form of BiOCl , thus achieving bismuth recovery. As shown in Figure 13,

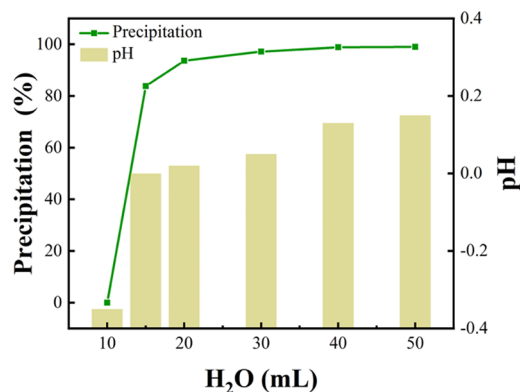


Figure 13. Effect of the added water dosage.

99.0% of Bi^{3+} was precipitated at a pH of 0.15. This can be attributed to the nitric acid used in the preceding step, which substantially reduced the Cl^- concentration in the solution. As illustrated in Figure 8, the decrease in the complexation reaction between Cl^- and Bi^{3+} led to an increased concentration of Bi^{3+} available for hydrolysis, ultimately causing Bi^{3+} to undergo hydrolysis at a lower pH. The XRD analysis presented in Figure 14 confirms that the precipitated bismuth phase is BiOCl (eq

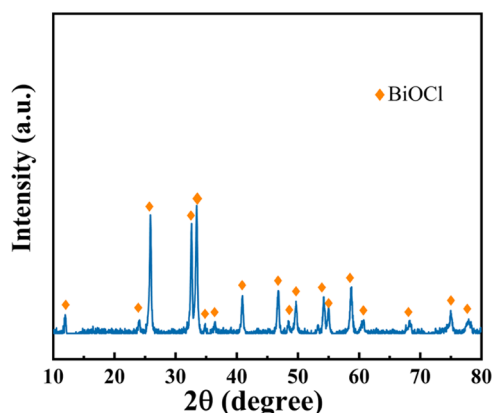
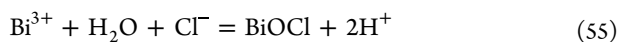


Figure 14. XRD patterns of precipitation.

55).²⁰ Previous calculations have demonstrated that tellurium does not undergo hydrolysis concurrently with bismuth precipitation in a low-pH environment. As a result, maintaining the pH below the threshold for tellurium hydrolysis throughout this process effectively minimizes tellurium impurities in the precipitated bismuth.



3.6. Scale-Up Experiment. The scale-up experiment was conducted in accordance with the experimental conditions and reagent quantities detailed in the previous sections. To the 50 g of bismuth telluride waste (Figure 15a), 250 mL of 12 mol/L

hydrochloric acid was added, followed by a slow addition of 33 wt % sodium chlorate solution. When 20 g of sodium chlorate was added, the bismuth telluride waste was almost entirely dissolved, resulting in a yellow transparent solution (Figure 15b). After the introduction of 5 g of hydroxylamine hydrochloride, the selenium removal process was completed through filtration (Figure 15c). The selenium-removed solution was then treated with sodium hydroxide and sodium sulfide, resulting in the precipitation of bismuth and antimony (Figure 15d) and tellurium leachate (Figure 15e). Following this, the pH of the leachate was adjusted to 5, yielding tellurium dioxide (Figure 15f). Subsequently, 35 mL of nitric acid was added, resulting in the formation of a bismuth leaching solution (Figure 15g) and the precipitation of antimony. Upon addition of an appropriate amount of water and NaOH to the bismuth leaching solution and adjustment of the pH to 0.15, bismuth oxychloride was hydrolyzed and precipitated (Figure 15h). The products from each stage were analyzed by ICP-OES, with the results presented in Table 5.

Table 5. Elemental Composition of the Products (ppm)

	Bi	Te	Se	Sb
dissolution solution	11 010	10 700	1989	528
post-selenium removal solution	11 000	10 657	0.6	529
post-tellurium removal solution	10 980	940.3	0.3	525
tellurium dioxide	2.2	9800	0.3	2
bismuth antimony precipitate	10 350	922.6	0.1	519
bismuth leaching solution	10 104	772.8	0.1	1.2
antimony precipitate	0.2	140	0.1	510
post-bismuth removal solution	12	732	0.1	1.9
bismuth oxychloride	10 080	10	0.1	0.8

Under the conditions of the scale-up experiment, the leaching efficiency of each element remained consistent. The process resulted in the recovery of 99.9% selenium, 99% antimony, and more than 90% tellurium. During the antimony–bismuth separation process, the increase in total mass led to a reduction in the relative loss of bismuth, achieving a bismuth separation percentage of 98% in the bismuth–antimony precipitate, surpassing 95.7% recorded in previous small-scale experiments. Additionally, due to the substantial differences in the hydrolysis capacities of tellurium and bismuth near a pH of 0.15, a large amount of impure tellurium was removed during the bismuth hydrolysis, ultimately yielding 99.9% purity for both tellurium and bismuth. Therefore, this method demonstrates excellent separation and purification of tellurium, bismuth, selenium, and antimony in discarded bismuth telluride waste. After the scale-up experiment, this method remains viable.

4. CONCLUSIONS

To separate and purify Te, Bi, Se, and Sb from bismuth telluride waste, this study investigates oxidative leaching with NaClO_3 , selenium reduction with hydroxylamine hydrochloride, tellurium separation through NaOH – Na_2S alkaline leaching, antimony separation with nitric acid, and bismuth precipitation via hydrolysis.

- (1) In the NaClO_3 oxidation process, 99.8% of bismuth telluride waste was dissolved and leached. The optimal reaction conditions were determined as follows: a NaClO_3 excess coefficient of 1.00 and a reaction temperature of 50 °C. After leaching, hydroxylamine

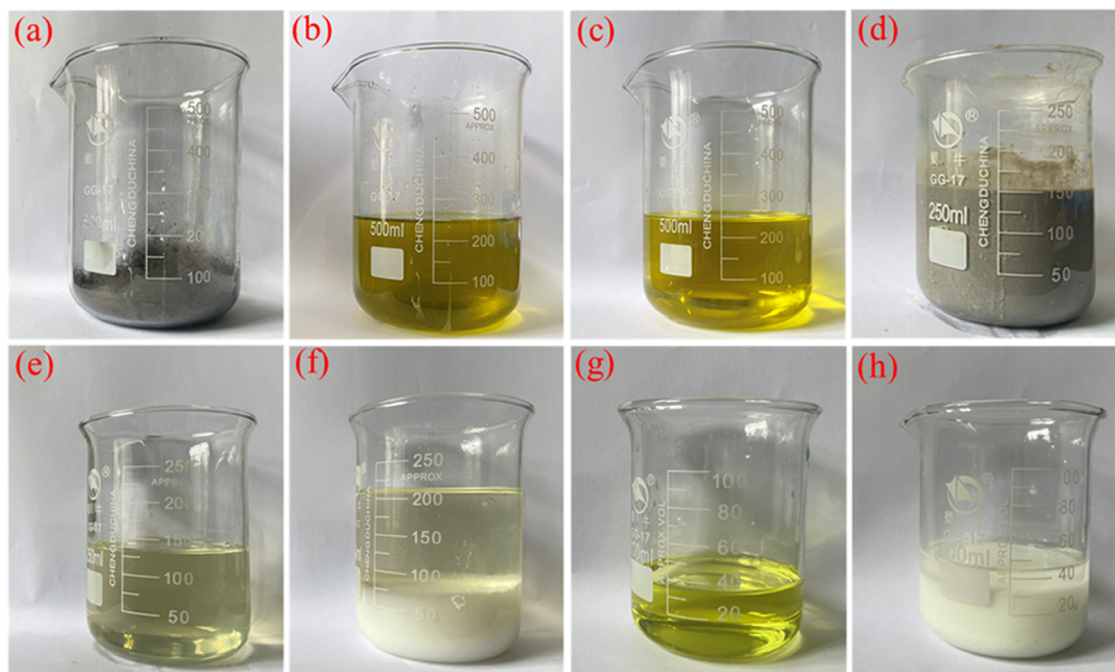


Figure 15. Products were obtained during the scale-up experiment.

hydrochloride at 5 times the selenium content was added, resulting in 99.9% selenium recovery by reduction.

- (2) During tellurium separation using NaOH–Na₂S alkaline leaching, an optimal NaOH excess coefficient of 1.25 and a Na₂S concentration of 1 g/L were selected. This approach decreased the precipitation percentage of tellurium from 11.9 to 7.5%. Additionally, direct tellurium recovery in the form of TeO₂ exceeded 90%, with the purity of TeO₂ achieving 99.9%. Additionally, over 99.9% of both antimony and bismuth was recuperated through precipitation.
- (3) In the antimony separation process using HNO₃, more than 95% of bismuth could be directly dissolved by adding HNO₃ to the Bi–Sb precipitate at a liquid–solid ratio of 1 mL/g, while antimony remained almost insoluble, enabling bismuth and antimony separation. Upon adjusting the pH of the obtained bismuth solution to 0.15, 98.9% of Bi³⁺ could be precipitated and recovered as BiOCl, with the purity of BiOCl reaching 99.9%.

■ AUTHOR INFORMATION

Corresponding Author

Gang Wang – College of Materials Science and Engineering, Sichuan University, Chengdu 610065, China; Email: electrowg100@scu.edu.cn

Authors

Jiangling Zhu – College of Materials Science and Engineering, Sichuan University, Chengdu 610065, China; orcid.org/0000-0002-2289-5429

Wenjun Zhu – College of Materials Science and Engineering, Sichuan University, Chengdu 610065, China

Linrui Ou – College of Materials Science and Engineering, Sichuan University, Chengdu 610065, China

Lin Zheng – Faculty of Metallurgical and Energy Engineering, Kunming University of Science and Technology, Kunming 650093, China

Jie Zhang – College of Materials Science and Engineering, Sichuan University, Chengdu 610065, China; orcid.org/0000-0003-3986-0238

Jinwei Chen – College of Materials Science and Engineering, Sichuan University, Chengdu 610065, China; orcid.org/0000-0003-4298-3749

Jingong Pan – CNBM (Chengdu) Optoelectronic Material Co., LTD., Chengdu 610065, China

Ruilin Wang – College of Materials Science and Engineering, Sichuan University, Chengdu 610065, China; orcid.org/0000-0003-3773-0886

Complete contact information is available at: <https://pubs.acs.org/10.1021/acsomega.3c04611>

Notes

The authors declare no competing financial interest.

■ ACKNOWLEDGMENTS

This work was supported by the Chengdu Technological Innovation R&D Project (2021-YF05-00482-SN, 2019-YF05-01836-SN), the Sichuan International Scientific and Technological Innovation Cooperation Project (2022YFH0039), the Special Fund for Strategic Cooperation between Sichuan University and Panzhihua City (2019CDPZH-2), and the Fundamental Research Funds for the Central Universities (2018SCUH0025).

■ REFERENCES

- (1) Kim, K. T.; Choi, S. Y.; Shin, E. H.; Moon, K. S.; Koo, H. Y.; Lee, G.-G.; Ha, G. H. The influence of CNTs on the thermoelectric properties of a CNT/Bi₂Te₃ composite. *Carbon* **2013**, *52*, 541–549.
- (2) Mamur, H.; Bhuiyan, M. R. A.; Korkmaz, F.; Nil, M. A review on bismuth telluride (Bi₂Te₃) nanostructure for thermoelectric applications. *Renewable Sustainable Energy Rev.* **2018**, *82*, 4159–4169.
- (3) Drabble, J. R.; Goodman, C. H. L. Chemical bonding in bismuth telluride. *J. Phys. Chem. Solids* **1958**, *5* (1), 142–144.

- (4) Lu, Y.; Xu, Z. Precious metals recovery from waste printed circuit boards: A review for current status and perspective. *Resour., Conserv. Recycl.* **2016**, *113*, 28–39.
- (5) Li, Z.; Qiu, F.; Tian, Q.; Yue, X.; Zhang, T. Production and recovery of tellurium from metallurgical intermediates and electronic waste—A comprehensive review. *J. Cleaner Prod.* **2022**, *366*, No. 132796.
- (6) Lee, J.-c.; Kurniawan, K.; Chung, K. W.; Kim, S. Metallurgical Process for Total Recovery of All Constituent Metals from Copper Anode Slimes: A Review of Established Technologies and Current Progress. *Met. Mater. Int.* **2021**, *27* (7), 2160–2187.
- (7) Sun, Z.-m.; Zheng, Y.-j. Preparation of high pure tellurium from raw tellurium containing Cu and Se by chemical method. *Trans. Nonferrous Met. Soc. China* **2011**, *21* (3), 665–672.
- (8) Zhang, F.-y.; Zheng, Y.-j.; Peng, G.-m. Selection of reductants for extracting selenium and tellurium from degoldized solution of copper anode slimes. *Trans. Nonferrous Met. Soc. China* **2017**, *27* (4), 917–924.
- (9) Fan, Y.; Yang, Y.; Xiao, Y.; Zhao, Z.; Lei, Y. Recovery of tellurium from high tellurium-bearing materials by alkaline pressure leaching process: Thermodynamic evaluation and experimental study. *Hydrometallurgy* **2013**, *139*, 95–99.
- (10) González-Ibarra, A.; Nava-Alonso, F.; Dávila-Pulido, G. I.; Carrillo-Pedroza, F. R.; Rodríguez-Flores, A. M. Dissolution behavior of elemental tellurium and tellurium dioxide in alkaline cyanide solutions. *Hydrometallurgy* **2021**, *203*, No. 105702.
- (11) Xu, S.; Wang, G.; Fan, J.; Wang, Z.; Zhang, J.; Chen, J.; Zheng, L.; Pan, J.; Wang, R. Preparation of high purity indium by chemical purification: Focus on removal of Cd, Pb, Sn and removal mechanism. *Hydrometallurgy* **2021**, *200*, No. 105551.
- (12) Yang, W.; Lan, X.; Wang, Q.; Dong, P.; Wang, G. Selective Pre-leaching of Tellurium From Telluride-Type Gold Concentrate. *Front. Chem.* **2021**, *9*, No. 593888.
- (13) Xu, Z.; Guo, X.; Li, D.; Tian, Q. Leaching kinetics of tellurium-bearing materials in alkaline sulfide solutions. *Miner. Process. Extr. Metall. Rev.* **2020**, *41* (1), 1–10.
- (14) Xu, Z.; Guo, X.; Li, D.; Tian, Q.; Zhu, L. Selective recovery of Sb and Te from the sodium sulfide leach solution of Te-bearing alkaline skimming slag by drop-wise H₂O₂ addition followed by Na₂S–Na₂SO₃ precipitation. *Hydrometallurgy* **2020**, *191*, No. 105219.
- (15) Zhong, J.; Wang, G.; Fan, J.; Li, Q.; Kiani, M.; Zhang, J.; Yang, H.; Chen, J.; Wang, R. Optimization of process on electrodeposition of 4N tellurium from alkaline leaching solutions. *Hydrometallurgy* **2018**, *176*, 17–25.
- (16) Fan, J.; Wang, G.; Xu, S.; Zhu, J.; Zhang, J.; Chen, J.; Zheng, L.; Pan, J.; Wang, R.; Hao, Y. Removal of impurities from bismuth pickling solution using solvent extraction with TBP. *Hydrometallurgy* **2022**, *207*, No. 105779.
- (17) Ling, H.; Malfliet, A.; Blanpain, B.; Guo, M. Selective removal of arsenic from crude antimony trioxide by leaching with nitric acid. *Sep. Purif. Technol.* **2022**, *281*, No. 119976.
- (18) Ajiboye, T. O.; Oyewo, O. A.; Onwudiwe, D. C. Simultaneous removal of organics and heavy metals from industrial wastewater: A review. *Chemosphere* **2021**, *262*, No. 128379.
- (19) Yao, G. L.; Shao, X.; Qiu, Z. W.; Qiu, F. X.; Li, Z. D.; Zhang, T. Construction of lignin-based nano-adsorbents for efficient and selective recovery of tellurium (IV) from wastewater. *Chemosphere* **2022**, *287*, No. 132058.
- (20) Hoffmann, J. E. Recovering selenium and tellurium from copper refinery slimes. *JOM* **1989**, *41* (7), 33–38.
- (21) Han, J.; Ou, Z.; Liu, W.; Jiao, F.; Qin, W. Recovery of antimony and bismuth from tin anode slime after soda roasting—alkaline leaching. *Sep. Purif. Technol.* **2020**, *242*, No. 116789.
- (22) Rhee, K.-I.; Lee, C. K.; Ha, Y.-C.; Jeong, G.-J.; Kim, H.-S.; Sohn, H.-J. Tellurium recovery from cemented tellurium with minimum waste disposal. *Hydrometallurgy* **1999**, *53* (2), 189–201.
- (23) Habashi, F. Arsenic, Antimony, and Bismuth Production. In *Encyclopedia of Materials: Science and Technology*, 2nd ed.; Elsevier, 2001; pp 332–336.
- (24) Ruirong, Z.; Xichang, S.; Hanying, J. Thermodynamic equilibrium of Sb-Cl-H₂O system. *Trans. Nonferrous Met. Soc. China* **1997**, *7* (4), 124–129.
- (25) Tian, Q.-h.; Xin, Y.-t.; Yang, L.; Wang, X.-h.; Guo, X.-y. Theoretical simulation and experimental study of hydrolysis separation of SbCl₃ in complexation–precipitation system. *Trans. Nonferrous Met. Soc. China* **2016**, *26* (10), 2746–2753.
- (26) Bard, A. J.; Parsons, R.; Jordan, J. *Standard Potentials in Aqueous Solution*; Routledge, 1985.
- (27) Zhang, L.; Guo, X.-y.; Tian, Q.-h.; Qin, H. Selective removal of arsenic from high arsenic dust in the NaOH-S system and leaching behavior of lead, antimony, zinc and tin. *Hydrometallurgy* **2021**, *202*, No. 105607.
- (28) Ajiboye, T. O.; Onwudiwe, D. C. Bismuth sulfide based compounds: Properties, synthesis and applications. *Results Chem.* **2021**, *3*, No. 100151.
- (29) Wikedzi, A.; Sandström, Å.; Awe, S. A. Recovery of antimony compounds from alkaline sulphide leachates. *Int. J. Miner. Process.* **2016**, *152*, 26–35.
- (30) Fan, J.; Wang, G.; Li, Q.; Yang, H.; Xu, S.; Zhang, J.; Chen, J.; Wang, R. Extraction of tellurium and high purity bismuth from processing residue of zinc anode slime by sulfation roasting-leaching-electrodeposition process. *Hydrometallurgy* **2020**, *194*, No. 105348.
- (31) Tereshatov, E. E.; Burns, J. D.; Vonder Haar, A. L.; Schultz, S. J.; McIntosh, L. A.; Tabacaru, G. C.; McCann, L. A.; Avila, G.; Hannaman, A.; Lofton, K. N.; et al. Separation, speciation, and mechanism of astatine and bismuth extraction from nitric acid into 1-octanol and methyl anthranilate. *Sep. Purif. Technol.* **2022**, *282*, No. 120088.